







PI coating expands, and this counteracts some of salinity-induced pressure, i.e., the pressure decreases and thus causes the spectrum blue shift. The bare FBG in the fiber loop is only sensitive to temperature. So temperature compensation can be achieved using the following matrix [12]:

$$\begin{bmatrix} \Delta T \\ \Delta S \end{bmatrix} = \frac{1}{K_{S,Sagnac} \cdot K_{T,FBG}} \begin{bmatrix} K_{S,Sagnac} & 0 \\ -K_{T,Sagnac} & K_{T,FBG} \end{bmatrix} \begin{bmatrix} \Delta\lambda_{FBG} \\ \Delta\lambda_{Sagnac} \end{bmatrix}, \quad (1)$$

where  $K_{S,Sagnac}$  and  $K_{T,Sagnac}$  are salinity and temperature sensitivities of the PI-coated Sagnac interferometer, respectively;  $K_{T,FBG}$  is the temperature sensitivity of the FBG.

### 3. Experimental results and discussion

#### 3.1 Salinity response

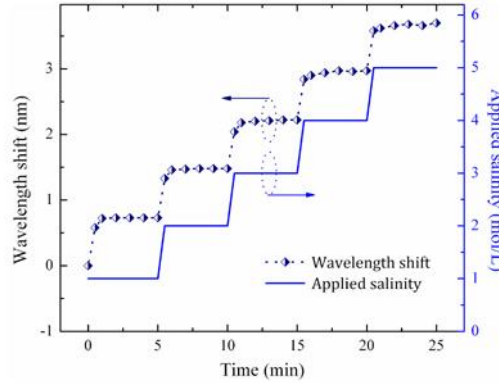


Fig. 2. Dynamic response of the sensor to change in water salinity.

The water tank was first filled with 100-mL of pure water. Saturated NaCl solution with a concentration of 5.5 mol/L was added to the water to vary the salinity of the solution. Solid NaCl was not used as it would take longer time to dissolve in water and would affect the measurement accuracy when characterizing the time response of the sensor. Figure 2 shows the time response of the Sagnac wavelength shift at different salinities. A fast response time of about one minute was measured for the sensor. Figure 3 (a) shows the output spectra of the sensor at different salinities. The FBG reflection wavelength peak remains unchanged when the salinity was varied from 0 mol/L to 5 mol/L, whereas the Sagnac interference minimum wavelengths shifted by about 3.736 nm. Figure 3 (b) shows the wavelength shift as a function of water salinity. Three measurements were carried out to verify its repeatability. Through a linear fitting, the salinity sensitivity of the PM-PCF Sagnac interferometer was found to be 0.742, 0.738 and 0.743 nm/M (M means mol/L for water salinity) for the three measurements, respectively, and that of the FBG is zero. This sensitivity is 45 times higher than the previous reported value of 0.0165 nm/M, which was based on a PI-coated FBG [12]. In addition, it is at least 6 times more sensitive than that of hydrogel-coated FBG [11]. One advantage of PI over hydrogel is its high temperature sustainability (up to 300 °C) and this makes our proposed salinity sensor suitable for harsh environment application. What's more, PI is widely used as fiber coating to enhance the mechanical strength of optical fibers for protection, which is crucial in engineering. Thus mature PI-recoater is commercially available, and such setup enables us fabricate PI coating with ease. However, for fabrication of hydrogel coating, it usually involves specially designed holder and UV-curing equipment, which is much more complex than the former.

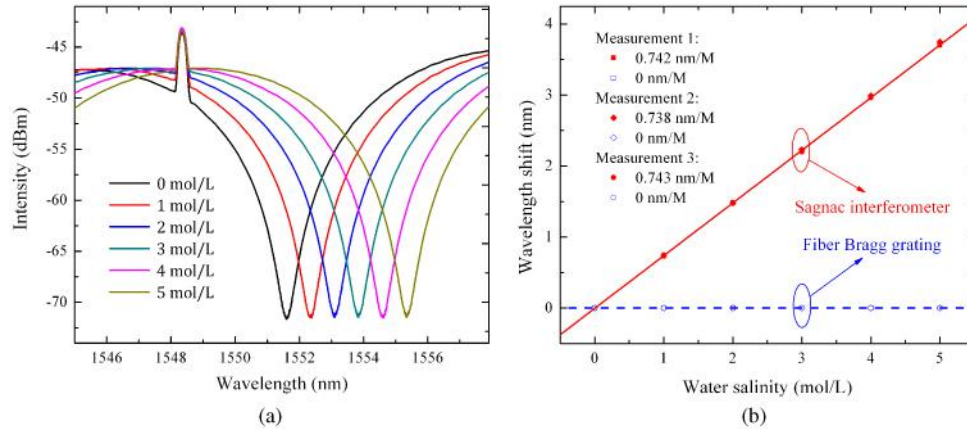


Fig. 3. (a) Spectra at different salinities for measurement 1. (b) Wavelength shift as a function of water salinity for three measurements.

To find out how salinity sensitivity depends on the length ( $L$ ) of PM-PCF, we consider the pressure sensitivity of a PM-PCF Sagnac interferometer. Refs [23] and [24] demonstrated that such interferometers with different  $L$ s showed similar pressure sensitivities. It can be expected that the PI-coated interferometers with different  $L$ s will also have similar salinity sensitivities since they are based on pressure effect of the coating. Note that the 20.8-cm PM-PCF we used is just an example, and the length of 20.8-cm is not a necessary value. The salinity sensitivity can be further improved by using a thicker PI coating at the expense of longer response time. A thicker coating will induce larger pressure and hence result in higher salinity sensitivity. However it will take longer time to response to ambient environmental change. Limited by the recoater, we can only fabricate PI coating with a maximum thickness of 18  $\mu\text{m}$ .

### 3.2 Temperature response and compensation

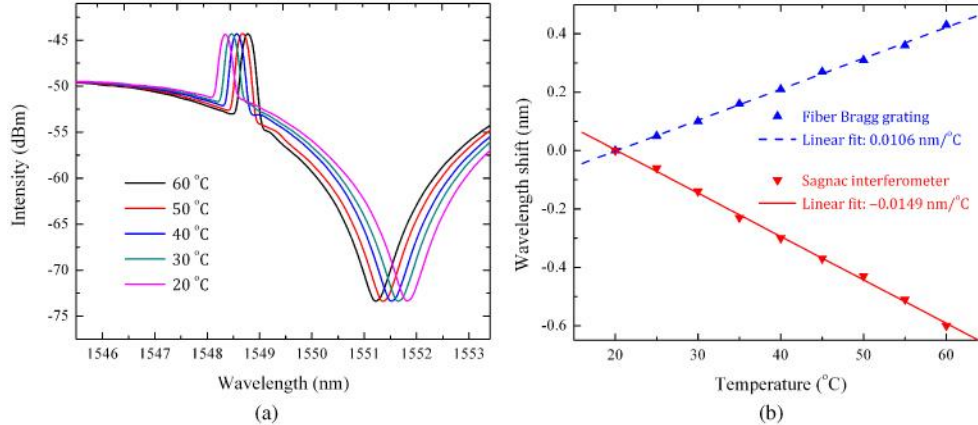


Fig. 4. (a) Spectra at different temperatures. (b) Wavelength shift as a function of temperature.

Temperature cross sensitivity of sensors is a big concern for real application since temperature fluctuation is inevitable in most applications and therefore affect the accuracy of the sensors. The sensor head was placed inside a hot water bath to investigate its temperature response. Data were collected when the temperature of the water bath was falling from 60  $^{\circ}\text{C}$  to 20  $^{\circ}\text{C}$  during the cooling-down process with steps of 5  $^{\circ}\text{C}$ . As shown in Fig. 4 (a) and (b), the FBG red shifts with a sensitivity of 0.0106  $\text{nm}/^{\circ}\text{C}$ , whereas the Sagnac interferometer blue shifts with a sensitivity of  $-0.0149 \text{ nm}/^{\circ}\text{C}$  which is at the same order of the grating based salinity

sensors [11, 12]. Hence, our sensor exhibits lower cross-sensitivity to temperature since it has much higher salinity sensitivity than that of the grating based sensors.

Using the salinity and temperature sensitivities obtained above, and substituting them to Eq. (1), temperature compensation can be performed using Eq. (2).

$$\begin{bmatrix} \Delta T \\ \Delta S \end{bmatrix} = \frac{1}{0.742 \times 0.0106} \begin{bmatrix} 0.742 & 0 \\ 0.0149 & 0.0106 \end{bmatrix} \begin{bmatrix} \Delta\lambda_{FBG} \\ \Delta\lambda_{Sagnac} \end{bmatrix}, \quad (2)$$

where  $\Delta\lambda_{FBG}$  and  $\Delta\lambda_{Sagnac}$  are in nm,  $\Delta T$  and  $\Delta S$  are obtained in °C and mol/L, respectively. Based on this equation, temperature and salinity can be simultaneously determined. To verify whether such a temperature compensation scheme works, we measured the water salinity at different temperatures using our sensor and the results are shown in Fig. 5. The standard deviations for the two measurements are 0.026 and 0.027 mol/L, which mainly come from the inaccuracy during data collection and the limitation of the OSA resolution (0.02 nm). The resolution of salinity measurement can be calculated as: 0.02 nm / 0.742 nm/(mol/L) = 0.027 mol/L, which is comparable with above error values.

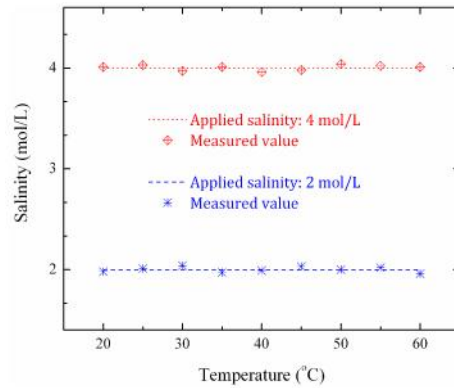


Fig. 5. Demonstration of temperature compensation for salinity measurements.

#### 4. Summary

In conclusion, we report a highly sensitive fiber-optic salinity sensor using a PI-coated PM-PCF Sagnac interferometer by exploiting the high pressure-sensitivity of the PM-PCF Sagnac interferometer and the coating swelling induced radial pressure effect on the fiber. This is the first time to exploit fiber coating induced pressure effect for salinity sensing. The achieved salinity sensitivity is 45 times higher than that of a PI-coated FBG. In addition, temperature compensation was successfully implemented by incorporating a bare FBG into the fiber loop. This fiber-optic salinity sensor features high sensitivity, compact size, ease for fabrication, and good thermal stability.

#### Acknowledgments

This work was supported in part by The Hong Kong Polytechnic University under the grant number G-YJ30, in part by the Key Project of National Natural Science Foundation of China (60736039), and in part by the Fundamental Research Funds for the Central Universities (21609102).